

# Quantum memory precludes mixed-unitary dynamics

Charlotte Bäcker,<sup>1</sup> Konstantin Beyer,<sup>2</sup> and Walter T. Strunz<sup>1</sup>

<sup>1</sup>*Institute of Theoretical Physics, TUD Dresden University of Technology, 01062, Dresden, Germany*

<sup>2</sup>*Department of Physics, Stevens Institute of Technology, Hoboken, New Jersey 07030, USA*

(Dated: 19th March 2026)

Unital quantum channels, defined by their property of leaving the maximally mixed state invariant, form an important class of quantum operations. A distinguished subset of these channels can be represented as a probabilistic mixture of unitary evolutions. Characterizing channels that do not admit such a decomposition is in general a hard problem with significant implications for noise mitigation in quantum technologies and for fundamental problems in quantum information theory. Here we establish a link between mixed-unitarity of unital channels and the (quantum) nature of the memory effects in non-Markovian dynamics. Translating the problem into the language of process tensors, this connection yields a hierarchy of semidefinite programs that provides numerically efficient witnesses for non-mixed-unitary behavior, outperforming existing criteria. We demonstrate the power of this approach through illustrative examples of unital channels in dimensions three and four.

*Introduction*— Unital quantum channels, i.e., those that preserve the identity,  $\mathcal{E}_u[\mathbb{1}] = \mathbb{1}$ , play a central role in many areas of quantum dynamics. They are relevant in resource theories [1–3] and are closely connected to concepts such as majorization and fluctuation theorems in quantum thermodynamics [4–7]. Furthermore, unital maps are crucial for noise modeling in the context of quantum computing. The dominant decoherence processes in quantum devices are often unital, as they occur on much shorter time scales than non-unital damping channels [8–11]. A particular class of unital channels are those of mixed-unitary type (MU)

$$\mathcal{E}_{\text{MU}}[\rho] = \sum_i p_i U_i \rho U_i^\dagger, \quad (1)$$

with the  $U_i$  being unitary and the  $p_i$  forming a probability distribution. Such channels describe unitary quantum dynamics with classical noise, and can be seen as the result of averaging over a Hamiltonian with a classical stochastic parameter, for example a random external field [12–14].

Finite-dimensional unital channels form a convex and compact set [15]. Thus, they can always be decomposed as

$$\mathcal{E}_u = \sum_i p_i \mathcal{E}_i^*, \quad p_i \geq 0, \quad \sum_i p_i = 1, \quad (2)$$

where the  $\mathcal{E}_i^*$  are the extreme points of the convex set. Any unitary is such an extreme point and for Hilbert spaces of dimension  $d = 2$  all of these extreme elements are unitary [16]. This implies that any unital channel on a qubit system is mixed-unitary.

It has long been known that this is no longer true for dimensions  $d \geq 3$ , where unital channels exist that do not admit an MU representation [16–20]. Various special classes of channels with this property have been proposed in the literature [15, 17–23], see also Fig. 1. However, generally applicable tools for the detection of unital channels that are non-MU are lacking and a broader characterization of such channels remains elusive. In fact, deciding whether a given unital channel is MU is an NP-hard problem [24]. Beyond mere academic interest in the features

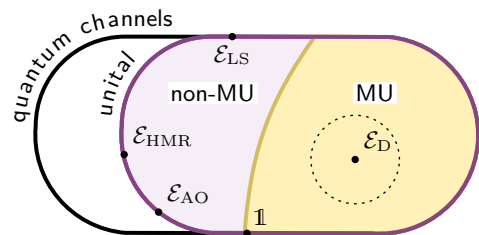


Figure 1. Geometric representation of the space of quantum channels with the five unital channels investigated thoroughly in this Letter being highlighted. Two of them are mixed-unitary (MU) and the other three channels are non-mixed-unitary (non-MU). Note that this two-dimensional depiction of the high-dimensional space of quantum channels does not capture all relevant properties, although convexity properties are reflected correctly.

of unital quantum channels, this question is of crucial practical relevance. It has been shown that MU channels always admit an environment-assisted error correction scheme that reverses the channel [25, 26]. This means that decoherence processes described by MU dynamics can, in principle, be mitigated perfectly. For unital channels that do not have an MU representation, such a correction scheme cannot exist [25]. This is sometimes called *truly quantum decoherence*, in contrast to a classical statistical mixture of unitary operations [19].

Recent developments have shown that qutrits, ququarts, and even higher-dimensional quantum systems may be beneficial for quantum computing [27–33], which makes the distinction between MU and non-MU noise processes directly relevant for error models and mitigation strategies. Moreover, in qubit-based devices, noise processes that act jointly on multiple qubits become increasingly relevant as single-qubit noise levels improve.

In this Letter, we address the problem of detecting non-MU unital channels from a rather surprising perspective. We map this problem to a recently developed framework for quantum memory in non-Markovian quantum dynamics [34]. The key insight is that since any MU dynam-

ics can be reversed by an environment-assisted scheme, such a reversal never necessitates quantum memory, as we will show below. Accordingly, witnesses of quantum memory in non-Markovian dynamics can be directly used to demonstrate non-MU behavior for a given quantum channel.

Building upon existing criteria for quantum memory [35], we provide numerical efficient methods, based on semidefinite programs (SDPs), for the detection of non-MU channels. We benchmark the method by showing that our witnesses outperform or match known criteria for various classes of qutrit non-MU channels in the literature. We then investigate a time-continuous joint dephasing process of a two-qubit system, showing that the unital evolution is non-MU at almost all times and therefore not correctable.

*Mapping to a quantum memory-related problem*— The field of non-Markovian quantum dynamics has long been an area of intense research. Recently, especially the origin of the memory effects has attracted much interest [34–43]. Following the definition in Refs. [34, 35] a two-step dynamics  $\mathcal{D} = (\mathcal{E}_1, \mathcal{E}_2)$  of two completely positive trace preserving maps (CPT maps) can be realized with a *classical memory* if these maps can be decomposed as

$$\mathcal{E}_2 = \sum_{\alpha} \mathcal{F}_{\alpha} \circ \mathcal{I}_{\alpha}, \quad \text{with} \quad \sum_{\alpha} \mathcal{I}_{\alpha} = \mathcal{E}_1, \quad (3)$$

where  $\mathcal{F}_{\alpha}$  is a family of CPT maps and the  $\mathcal{I}_{\alpha}$  form a quantum instrument. The reasoning behind this definition is that the dynamics can be decomposed into a measurement described by  $\mathcal{I}_{\alpha}$  for the first map  $\mathcal{E}_1$ , followed by a CPT channel  $\mathcal{F}_{\alpha}$  that is conditioned on the *classical* measurement outcome  $\alpha$ . If such a decomposition does not exist, the dynamics is said to require *truly quantum memory* (see Ref. [34] for details). Based on this definition the following theorem can be formulated:

**Theorem 1.** *A unital map  $\mathcal{E}_u$  is mixed-unitary if and only if the dynamics  $\mathcal{D} = (\mathcal{E}_u, \mathbb{1})$  is realizable with classical memory.*

*Proof* For the special case of a dynamics  $\mathcal{D} = (\mathcal{E}_1, \mathcal{E}_2)$  with  $\mathcal{E}_1 = \mathcal{E}_u$  and  $\mathcal{E}_2 = \mathbb{1}$ , the definition of classical memory in Eq. (3) reduces to a form that is identical to the existence of an environment-assisted error correction scheme in the sense of Ref. [25] whose equivalence to  $\mathcal{E}_u$  being MU has been established in said reference (see App. A for details and App. B for a corollary). ■

Intuitively, the connection can be understood by the fact that if  $\mathcal{E}_1$  is a mixture of unitary channels then the  $\mathcal{F}_{\alpha}$  can be chosen to be the corresponding inverse unitary operations, thus restoring the initial quantum state. A correction scheme as in Ref. [25] exists exactly then when the measurement outcomes can be used to perfectly reverse the channel  $\mathcal{E}$ , i.e. if the second map in the dynamics is the identity.

Having established the equivalence between  $\mathcal{E}_u$  being non-MU and  $\mathcal{D} = (\mathcal{E}_u, \mathbb{1})$  being a dynamics that requires

quantum memory, we can employ the existing criteria for the latter to demonstrate the former. The Choi state  $E$  of a completely positive map  $\mathcal{E}$  is defined through the Choi-Jamiołkowski isomorphism

$$E = (\mathbb{1} \otimes \mathcal{E})|\Phi^+\rangle\langle\Phi^+|, \quad (4)$$

with the unnormalized Bell state  $|\Phi^+\rangle = \sum_{k=0}^{d-1} |k\rangle \otimes |k\rangle$ . In Ref. [34] it was shown that a dynamics  $\mathcal{D} = (\mathcal{E}_1, \mathcal{E}_2)$  requires quantum memory if

$$\varepsilon^{\sharp}[E_1] < \varepsilon[E_2], \quad (5)$$

where  $\varepsilon^{\sharp}$  and  $\varepsilon$  denote the entanglement of assistance [44, 45] and entanglement of formation [46, 47], respectively, and  $E_{1,2}$  are the Choi states of the maps  $\mathcal{E}_{1,2}$ . We note that for the special case  $\mathcal{E}_2 = \mathbb{1}$ , considered here, the criterion Eq. (5) becomes tight (see App. C).

The entanglement of assistance is an NP-hard quantity [24] and thus the quantum memory criterion in Eq. (5) is not computationally helpful to detect non-MU channels. However, the equivalence established in Th. 1 now allows us to apply all the tools developed in the context of quantum memory theory. In particular, in Ref. [35] the definition of classical memory has been relaxed to an SDP which serves as a witness for quantum memory. It hence eliminates the possibility of a representation with classical memory and can be used to identify non-MU channels. This is very similar to approaches certifying entanglement by using the convexity of the class of separable states [48–50].

*SDP non-MU witnesses*— A dynamics  $\mathcal{D} = (\mathcal{E}_1, \mathcal{E}_2)$  can always be regarded as emerging from a process tensor in Choi representation  $X^{AB'BC'}$ , which can be interpreted as a four-partite quantum state [51]. Here the Hilbert space  $A$  describes the input at time  $t_0$ ,  $B'$  is the output Hilbert space at time  $t_1$ ,  $B$  is the input Hilbert space for the second time step, and  $C'$  the output Hilbert space at time  $t_2$ . For  $X$  to be compatible with the dynamics, it must reproduce the correct Choi states  $E_{1,2}$  of the maps  $\mathcal{E}_{1,2}$ :

$$\text{tr}_{C'}[X^{AB'BC'}] = E_1 \otimes \mathbb{1}_B, \quad (6)$$

$$\langle\Phi_{B'B}^+| X^{AB'BC'} |\Phi_{B'B}^+\rangle = E_2. \quad (7)$$

In general, there are infinitely many  $X$  that yield the dynamics  $\mathcal{D} = (\mathcal{E}_1, \mathcal{E}_2)$ . However, if a dynamics admits a classical memory decomposition as in Eq. (3), there is at least one separable realization of the form [35]

$$X^{AB'BC'} = \sum_{\alpha} I_{\alpha}^{AB'} \otimes F_{\alpha}^{BC'}, \quad (8)$$

where  $I_{\alpha}$  and  $F_{\alpha}$  are the Choi states of  $\mathcal{I}_{\alpha}$  and  $\mathcal{F}_{\alpha}$ , respectively [see Eq. (4)].

Accordingly, if a unital map  $\mathcal{E}_u$  is MU, all process tensors that are compatible with the dynamics  $\mathcal{D} = (\mathcal{E}_u, \mathbb{1})$  must be separable with respect to the partition  $AB'|BC'$ . Since separability is an NP-hard problem as well [52], this

framing of the problem does not simplify the problem directly. However, based on the Doherty-Parrilo-Spedalieri (DPS) hierarchy [49, 50], the question of separability can be cast into a hierarchy of semidefinite programs (SDP). The first level of this hierarchy is the Peres-Horodecki or positive-partial-transpose (PPT) criterion [48] verifying entanglement, which was used in Ref. [35] for the case of quantum memory detection. Adapted for our case of non-MU detection we can formulate the following SDP:

$$s_{\text{QM}} = \max_X \left( \frac{1}{d^2} \langle \Phi^+ | G | \Phi^+ \rangle - 1 \right), \quad (9)$$

$$\text{s.t.}: X^{AB'BC'} \succeq 0, \quad (10)$$

$$(X^{AB'BC'})^{\top}_{BC'} \succeq 0, \quad (11)$$

$$\text{tr}_{C'}[X_{AB'BC'}] = E_u \otimes \mathbb{1}_B, \quad (12)$$

$$G = \langle \Phi^+_{B'B} | X^{AB'BC'} | \Phi^+_{B'B} \rangle. \quad (13)$$

The constraints describe the positivity of  $X$  (10) and its partial transpose (11), the marginal for the first channel which has to agree with the unital channel  $\mathcal{E}_u$  whose non-MU property we are interested (12), and the second marginal which we denote by  $G$  (13). The fidelity of this marginal  $G$  with the expected Choi state of the identity map  $E_2 = |\Phi^+\rangle\langle\Phi^+|$  is maximized in the objective function of the SDP (9) (note the scaling by  $d^2$  due to the unnormalized Choi states). If the maximum  $s_{\text{QM}}$  is negative, the dynamics  $\mathcal{D} = (\mathcal{E}_u, \mathbb{1})$  cannot be realized with a separable process tensor  $X$ , hence,  $\mathcal{E}_u$  is of non-MU form. Thus,  $s_{\text{QM}}$  is a non-MU witness.

The PPT constraint in Eq. (11) leads to a sufficient but not necessary witness. Stronger witnesses can be obtained by adding further PPT constraints for symmetric extensions of the Hilbert space of  $X$  to the SDP. In theory such a DPS hierarchy is guaranteed to converge in the limit of infinite depth [49].

In practice, even small depths are computationally costly. However, already the first order, given above, often provides a strong witness. In the following sections we analyze the performance of this non-MU witness on different exemplary classes of unital channels. Most examples are concerned with the qutrit case  $d = 3$  as the lowest dimension in which the question of MU vs. non-MU channels is non-trivial. We compare the results with previously reported criteria in the literature, showing that our witness can detect the non-MU behavior in significantly larger parameter regions (see Fig. 3 for an overview). In App. D we provide further witnesses that are in general weaker than Eq. (9) but can be numerically more efficient and adapted to measurable observables in an experimental setup.

*The Landau-Streater channel ( $d = 3$ )*— It is known that unital qutrit dynamics of Kraus rank  $r = 2$  are always MU. For channels of rank  $r \geq 3$  this is no longer true. The prototypical qutrit channel which does not allow for a representation in terms of a mixture of unitary dynamics is the so-called *Landau-Streater* (LS) channel  $\mathcal{E}_{LS}$ , given

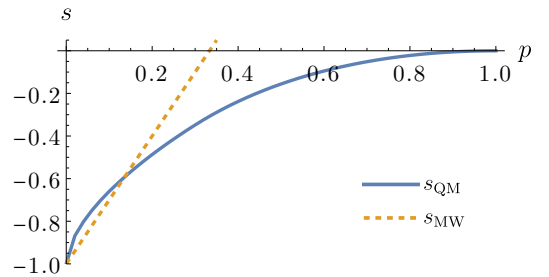


Figure 2. Witnesses of non-mixed-unitaryness in the family of CPT maps given by Eq. (15). The blue solid line represents the quantum-memory-based witness  $s_{\text{QM}}$  and indicates non-mixed-unitaryness if it is negative. The orange dashed line computed the witness  $s_{\text{MW}}$  according Eq. (16) indicates non-mixed-unitaryness if the value is below zero, which is the case for all  $p < 1/3$ . Both witnesses are normalized to  $s = -1$  at  $p = 0$ .

in terms of the following Kraus representation [16, 17]

$$\begin{aligned} K_1 &= |1\rangle\langle 2| - |2\rangle\langle 1|, & K_2 &= |0\rangle\langle 2| - |2\rangle\langle 0|, \\ K_3 &= |0\rangle\langle 1| - |1\rangle\langle 0|. \end{aligned} \quad (14)$$

Mixing this channel with the identity channel, we define a family of channels

$$\mathcal{E}_p = p\mathbb{1} + (1-p)\mathcal{E}_{LS}, \quad p \in [0, 1]. \quad (15)$$

In Ref. [23] it was shown analytically that this family possesses a MU representation only in the trivial case  $p = 1$ . This result serves as a first benchmark for our quantum memory-based non-MU witness. In Fig. 2 we plot the optimized fidelity  $s_{\text{QM}}$  [see Eq. (9)] as a function of the mixing parameter  $p$  in Eq. (15), showing that the witness correctly detects the non-MU behavior for all  $p < 1$ .

Previously known criteria for the non-MU nature of unital channels usually only apply to a certain specific class with high symmetry. One generally applicable witness for non-MU qutrit channels was proposed by Mendl and Wolf [15]. They show that a unital qutrit channel  $\mathcal{E}_u$  is non-MU if its Choi state  $E_u$  satisfies

$$s_{\text{MW}} = \text{tr}[WE_u] < 0, \quad (16)$$

with

$$W = \frac{1}{3}(3\mathbb{F} + \mathbb{1}), \quad \mathbb{F} : |k, l\rangle \mapsto |l, k\rangle. \quad (17)$$

The Mendl-Wolf criterion serves as numerical benchmark for our witness  $s_{\text{QM}}$ . We plot  $s_{\text{MW}}$  in Fig. 2 for comparison. The Mendl-Wolf witness detects the true nature of the family only for  $p < 1/3$ . Thus, our witness performs significantly better for the channels  $\mathcal{E}_p$  in Eq. (15).

*Convex mixtures of extremal channels*— For the 80-dimensional space of qutrit channels it is known that unital channels form a convex subset and therein mixed-unitary channels form another convex subset of non-zero volume [21]. One important observation is the fact that the subset of non-MU channels is not convex (see App. E).

In order to demonstrate the versatility of the quantum memory-based approach to the certification of non-MU channels, we analyze pairwise convex combinations of five different unital qutrit channels. Two of them, the identity map  $\mathbb{1}$  and the fully depolarizing channel  $\mathcal{E}_D$ , are of MU form. The other three are known to be non-MU: the Landau-Streater-channel  $\mathcal{E}_{LS}$  [16, 17], the Arveson-Ohno-Channel  $\mathcal{E}_{AO}$  [18, 20], and one channel  $\mathcal{E}_{HMR}$  of the Haagerup-Musat-Ruskai family [20]. Apart from the depolarizing channel  $\mathcal{E}_D$ , all of them are extreme points of the set of unital channels (see Fig. 1). Details on the definition and further properties of these channels can be found in App. F.

For most of those convex combinations no analytical results exist and we hence compare the performance of our witness  $s_{QM}$  in (9) with the witness  $s_{MW}$  from Eq. (17). The results are visualized in Fig. 3. Both witnesses detect the same parameter range for the non-MU behavior of the channel  $\mathcal{E}_{LS}$  mixed with a fully depolarizing channel. For all other convex combinations, the quantum-memory-based witness  $s_{QM}$  is able to demonstrate the non-MU property in a larger parameter region than the witness  $s_{MW}$ .

*Genuine quantum decoherence of a four-level system*—

For a single qubit every unital channel is MU and therefore qubit decoherence processes can in principle always be corrected by a measure and feedback scheme on the environment [25]. This is no longer true for a multi-qubit system that couples jointly to its surrounding. Here we analyze the non-MU detection of our quantum-memory based witness for the prototypical case of this class: a two-qubit system that experiences a non-Markovian dephasing dynamics. A model that produces such an evolution is shown in Fig. 4. The two system qubits couple to a single environmental qubit which in turn is damped by a Markovian channel.

The global evolution of an initial product state  $\rho(0) = \rho_{\text{sys}}(0) \otimes \rho_{\text{env}}(0)$  is determined by the three-qubit Hamiltonian  $H = H_{\text{int}} + H_{\text{env}}$  with

$$H_{\text{int}} = \kappa_1(\sigma_z^{\text{sys},1} \otimes \sigma_z^{\text{env}}) + \kappa_2(\sigma_z^{\text{sys},2} \otimes \sigma_z^{\text{env}}) \quad (18)$$

and  $H_{\text{env}} = \vec{\sigma} \vec{\Gamma}$ . Here, the  $\kappa_i$  are the interaction strengths between the single system qubit  $i$  and the environmental qubit. The  $\Gamma_i \in \mathbb{R}$  determine the direction of the Pauli noise in terms of the Pauli vector  $\vec{\sigma} = (\sigma_x, \sigma_y, \sigma_z)$  on the environmental qubit. We can add an irreversibility of strength  $\gamma$  by coupling the environmental qubit to a bath via a GKSL master equation [53, 54] with Lindblad operator  $L = \sigma_- = |0\rangle\langle 1|$ . The dynamics is thus determined by

$$\dot{\rho} = -i[H, \rho] + \mathcal{L}[\rho], \quad (19)$$

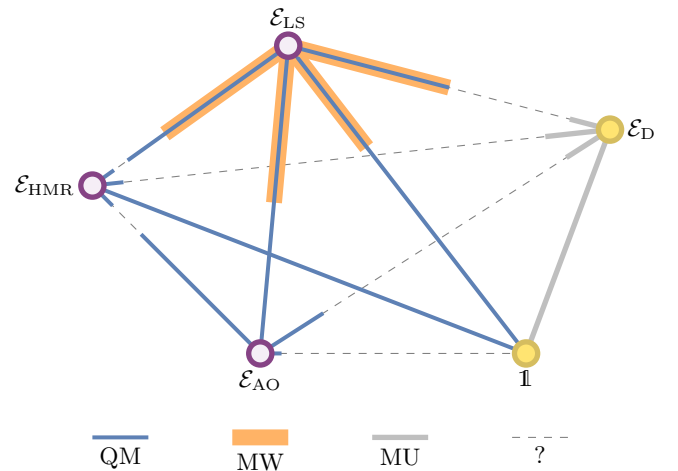


Figure 3. Overview of the performance of the quantum memory witness (QM) and the Mendl-Wolf witness (MW) for convex combinations of different unital channels. The three channels  $\mathcal{E}_{LS}$ ,  $\mathcal{E}_{AO}$  and  $\mathcal{E}_{HMR}$  are verifiably non-MU while the fully depolarizing channel  $\mathcal{E}_D$  and the identity channel  $\mathbb{1}$  have known MU decompositions. It can be seen that for the convex combination of  $\mathcal{E}_{LS}$  and  $\mathcal{E}_D$  the QM witness (blue thin line) performs equally well as the Mendl-Wolf-witness (orange thick line), while it outperforms the latter one in every other of the investigated convex combinations. The solid gray lines indicate parameter ranges for which it is known that the channel is MU [21] while dashed gray lines indicate parameter ranges for which nothing can be concluded from the witnesses. The details and parameter ranges depicted in this figure can be found in App. G in Tab. I.

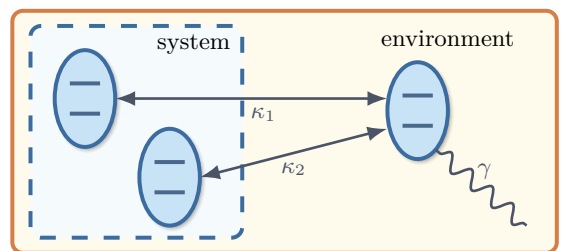


Figure 4. Setting to realize irreversible unital two-qubit dynamics. The system-environment interaction is described by Eqs. (18) and (19).

with  $\mathcal{L}[\rho] = \gamma [L\rho L^\dagger/2 - (L^\dagger L\rho + \rho L^\dagger L)]$ . Tracing over the environmental qubit, this leads to a non-Markovian unital decoherence process of the two-qubit system.

We can now investigate this model with respect to the property of being non-MU. Note that an extension of the Mendl-Wolf criterion in Eq. (17) to even dimensions leads to a trivial witness  $s_{MW}$  [15] and is, thus, not applicable to the case  $d = 4$  considered here.

Our witness in Eq. (9) does detect the non-MU nature of the joint two-qubit dynamics. The results for different damping strengths  $\gamma$  are shown in Fig. 5. The SDP to witness non-MU dynamics certifies that for large parameter ranges this model has no mixed-unitary representation. In

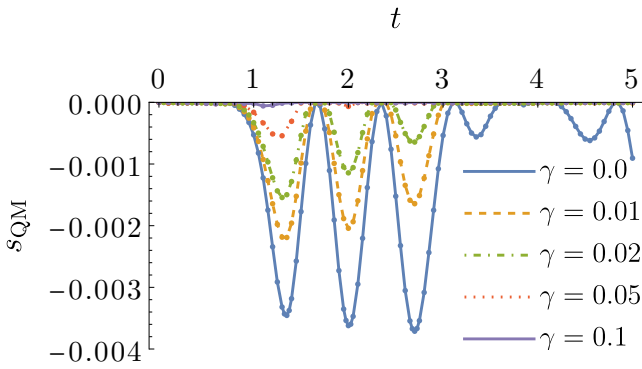


Figure 5. Non-MU witness from Eq. (9) applied to the dynamics in Fig. 4. The parameters  $\kappa_1 = 0.4$ ,  $\kappa_2 = 1.2$ ,  $\Gamma_x = 0.4$ ,  $\Gamma_y = 0$  and  $\Gamma_z = 1.0$  are chosen such that the dynamics has no mixed-unitary representation for almost all times [19].

contrast to the advances on witnessing the truly quantum nature of decoherence processes in  $d = 4$  from for example Ref. [19] the quantum memory-based witness features multiple advantages. It does neither rely on knowledge of the exact dynamics of the environment, nor is it limited to the particular Kraus rank  $r = 2$ . Furthermore, the SDP ensures that the computation is not as numerically involved as previous approaches. Therefore, the quantum-memory-based formulation using a numerically efficient semidefinite program is a very helpful tool in the context of ququarts. Note that for  $s = 0$ , however, we cannot make statements about the nature of the noise, the dynamics could or could not be mixed-unitary. Numerically involved further considerations of the next steps in the DPS-hierarchy [49, 50] could refine these results.

*Conclusion*— Determining whether a unital quantum channel admits a mixed-unitary representation is a problem of both fundamental and practical importance, yet re-

mains hard in general. In this Letter we have presented an efficient method to exclude the existence of mixed-unitary representations by establishing a fundamental connection to quantum memory criteria in non-Markovian dynamics. Mapping the problem to the identification of separable process tensors, we obtain a hierarchy of semidefinite programs that, in principle, fully characterizes the set of mixed-unitary channels. Already the lowest level of this hierarchy yields strong witnesses, as demonstrated for multiple prototypical classes of unital qutrit channels, where our approach compares favorably to existing methods. We further showed that for a time-continuous joint dephasing dynamics of a two-qubit system, the witness detects non-mixed-unitary behavior at almost all times.

The connection between quantum memory and mixed-unitarity extends well beyond the specific witnesses constructed here. Any advance in detecting quantum memory—an active area of research—translates directly into new tools for characterizing unital channels, making the framework naturally extensible. From a practical standpoint, the witnesses are readily adaptable to experimental constraints, and can often be tailored to measurement settings available in a given setup. As truly quantum decoherence processes described by non-mixed-unitary channels represent a central challenge for noise mitigation in emerging quantum technologies, we expect our framework to find broad application in the characterization and benchmarking of realistic quantum devices.

## ACKNOWLEDGEMENTS

C. B. acknowledges support by the German Academic Scholarship Foundation. K. B. acknowledges support by the NSF under award No. 2239498, NASA under award No. 80NSSC25K7051 and the Sloan Foundation under award No. G-2023-21102.

- 
- [1] E. Chitambar and G. Gour, *Rev. Mod. Phys.* **91**, 025001 (2019).
  - [2] G. Gour, M. P. Müller, V. Narasimhachar, R. W. Spekkens, and N. Yunger Halpern, *Phys. Rep.* **583**, 1 (2015).
  - [3] A. Streltsov, H. Kampermann, S. Wölk, M. Gessner, and D. Bruß, *New. J. Phys.* **20**, 053058 (2018).
  - [4] J. Watrous, “Unital channels and majorization,” in *The Theory of Quantum Information* (Cambridge University Press, 2018) p. 201–249.
  - [5] J. de Boer, G. Di Giulio, E. Keski-Vakkuri, and E. Tonni, *Phys. Rev. A* **112**, 032405 (2025).
  - [6] A. E. Rastegin, *J. Stat. Mech.: Theory Exp.* **2013**, P06016 (2013).
  - [7] T. Albash, D. A. Lidar, M. Marvian, and P. Zanardi, *Phys. Rev. E* **88**, 032146 (2013).
  - [8] T. D. Ladd, F. Jelezko, R. Laflamme, Y. Nakamura, C. Monroe, and J. L. O’Brien, *Nature* **464**, 45 (2010).
  - [9] D. Suter and G. A. Álvarez, *Reviews of Modern Physics* **88**, 041001 (2016).
  - [10] E. Paladino, Y. M. Galperin, G. Falci, and B. L. Altshuler, *Reviews of Modern Physics* **86**, 361 (2014).
  - [11] P. Krantz, M. Kjaergaard, F. Yan, T. P. Orlando, S. Gustavsson, and W. D. Oliver, *Applied Physics Reviews* **6**, 021318 (2019).
  - [12] R. Alicki, *Quantum Dynamical Semigroups and Applications*, 2nd ed., Lecture Notes in Physics Ser No. v.717 (Springer, Berlin, Heidelberg, 2007).
  - [13] J. Helm and W. T. Strunz, *Phys. Rev. A* **81**, 042314 (2010).
  - [14] A. A. Budini, *Phys. Rev. E* **72**, 056106 (2005).
  - [15] C. B. Mendl and M. M. Wolf, *Commun. Math. Phys.* **289**, 1057 (2009).
  - [16] L. J. Landau and R. F. Streater, *Lin. Alg. Appl.* **193**, 107 (1993).
  - [17] B. Kümmerer and H. Maassen, *Communications in Mathematical Physics* **109**, 1 (1987).

- [18] H. Ohno, *J. Math. Phys.* **51**, 092101 (2010).
- [19] J. Helm and W. T. Strunz, *Phys. Rev. A* **80**, 042108 (2009).
- [20] U. Haagerup, M. Musat, and M. B. Ruskai, *Annales Henri Poincaré* **22**, 3455 (2021).
- [21] J. Watrous, *Quantum Inf. Comput.* **9**, 406 (2009).
- [22] C. Rodríguez-Ramos and C. M. Wilmott, *J. Phys. A-Math.* **56**, 455308 (2023).
- [23] D. W. Kribs, J. Levick, R. Pereira, and M. Rahaman, *J. Phys. A-Math.* **57**, 115303 (2024).
- [24] C. D.-Y. Lee and J. Watrous, *Quantum* **4**, 253 (2020), 1902.03164.
- [25] M. Gregoratti and R. F. Werner, *J. Mod. Opt.* **50**, 915 (2003).
- [26] B. Trendelkamp-Schroer, J. Helm, and W. T. Strunz, *Phys. Rev. A* **84**, 062314 (2011).
- [27] B. P. Lanyon, M. Barbieri, M. P. Almeida, T. Jennewein, T. C. Ralph, K. J. Resch, G. J. Pryde, J. L. O'Brien, A. Gilchrist, and A. G. White, *Nature Physics* **5**, 134 (2009).
- [28] A. Fedorov, L. Steffen, M. Baur, M. P. da Silva, and A. Wallraff, *Nature* **481**, 170 (2012).
- [29] Z. Gedik, I. A. Silva, B. Çakmak, G. Karpát, E. L. G. Vidoto, D. O. Soares-Pinto, E. R. deAzevedo, and F. F. Fanchini, *Scientific Reports* **5**, 14671 (2015).
- [30] M. Ringbauer, M. Meth, L. Postler, R. Stricker, R. Blatt, P. Schindler, and T. Monz, *Nature Physics* **18**, 1053 (2022).
- [31] T. Roy, Z. Li, E. Kapit, and D. Schuster, *Phys. Rev. Appl.* **19**, 064024 (2023).
- [32] A. Pavlidis and E. Floratos, *Phys. Rev. A* **103**, 032417 (2021).
- [33] L. M. Seifert, Z. Li, T. Roy, D. I. Schuster, F. T. Chong, and J. M. Baker, *Phys. Rev. A* **108**, 062609 (2023).
- [34] C. Bäcker, K. Beyer, and W. T. Strunz, *Phys. Rev. Lett.* **132**, 060402 (2024).
- [35] M. Yu, T.-A. Ohst, H.-C. Nguyen, and S. Nimmrichter, (2025), arXiv:2504.08605 [quant-ph].
- [36] S. Milz, D. Egloff, P. Taranto, T. Theurer, M. B. Plenio, A. Smirne, and S. F. Huelga, *Phys. Rev. X* **10**, 041049 (2020).
- [37] C. Giarmatzi and F. Costa, *Quantum* **5**, 440 (2021).
- [38] M. Banacki, M. Marciniak, K. Horodecki, and P. Horodecki, *Phys. Rev. A* **107**, 032202 (2023).
- [39] P. Taranto, M. T. Quintino, M. Muraò, and S. Milz, *Quantum* **8**, 1328 (2024).
- [40] F. Buscemi, R. Gangwar, K. Goswami, H. Badhani, T. Pandit, B. Mohan, S. Das, and M. N. Bera, *PRX Quantum* **6**, 020316 (2025).
- [41] K. Goswami, A. K. Roy, V. Srivastava, B. Perez, C. Giarmatzi, A. Gilchrist, and F. Costa, *New Journal of Physics* **27**, 114515 (2025).
- [42] C. Bäcker, K. Beyer, and W. T. Strunz, *Phys. Rev. Res.* **7**, 033256 (2025).
- [43] C. Bäcker, V. Link, and W. T. Strunz, *Phys. Rev. Res.*, (2025).
- [44] D. P. DiVincenzo, C. A. Fuchs, H. Mabuchi, J. A. Smolin, A. Thapliyal, and A. Uhlmann, in *Quantum Computing and Quantum Communications*, Lecture Notes in Computer Science, edited by C. P. Williams (Springer, Berlin, Heidelberg, 1999) pp. 247–257.
- [45] T. Laustsen, F. Verstraete, and S. V. Enk, *Quantum Inf. Comput.* **3** (2002).
- [46] S. A. Hill and W. K. Wootters, *Phys. Rev. Lett.* **78**, 5022 (1997).
- [47] W. K. Wootters, *Phys. Rev. Lett.* **80**, 2245 (1998).
- [48] R. Simon, *Phys. Rev. Lett.* **84**, 2726 (2000).
- [49] A. C. Doherty, P. A. Parrilo, and F. M. Spedalieri, *Phys. Rev. Lett.* **88**, 187904 (2002).
- [50] A. C. Doherty, P. A. Parrilo, and F. M. Spedalieri, *Phys. Rev. A* **69**, 022308 (2004).
- [51] F. A. Pollock, C. Rodríguez-Rosario, T. Frauenheim, M. Paternostro, and K. Modi, *Physical Review A* **97**, 012127 (2018).
- [52] S. Gharibian, *Quantum Inf. & Comput.* **10**, 343–360 (2010).
- [53] V. Gorini, A. Kossakowski, and E. C. G. Sudarshan, *J. Math. Phys.* **17**, 821 (1976).
- [54] G. Lindblad, *Commun. Math. Phys.* **48**, 119 (1976).
- [55] K. M. R. Audenaert and S. Scheel, *New J. Phys.* **10**, 023011 (2008).
- [56] V. Karimipour, *Phys. Rev. A* **110**, 022424 (2024).

## Appendix A: Proof of Th. 1

*Proof.* For the details on the proof of Th. 1, let us first compare the definition of a dynamics  $\mathcal{D} = (\mathcal{E}, \mathcal{E}_2)$  with CPT maps  $\mathcal{E}, \mathcal{E}_2$  having classical memory with the definition of a correction scheme restoring quantum information for a map  $T$ . Such a scheme leading to the corrected channel  $T_{\text{corr}}$  is defined as [25]

$$T_{\text{corr}} = \sum_{\alpha} R_{\alpha} \circ T_{\alpha}, \quad \sum_{\alpha} T_{\alpha} = T, \quad (\text{A1})$$

where the  $R_{\alpha}$  represent a family of CPT maps. The similarity between Eq. (3) and Eq. (A1) becomes obvious once one identifies

$$\mathcal{E} \equiv T, \quad \mathcal{E}_2 \equiv T_{\text{corr}}, \quad \mathcal{I}_{\alpha} \equiv T_{\alpha}, \quad \mathcal{F}_{\alpha} \equiv R_{\alpha}. \quad (\text{A2})$$

There is hence a one-to-one correspondence between dynamics with classical memory and those with correction schemes. We will now show that  $\mathcal{E}$  being MU is the same as  $\mathcal{D} = (\mathcal{E}, \mathbb{1})$  having classical memory which again is equivalent to the existence of a scheme restoring quantum information for  $\mathcal{E}$ .

Given some dynamics  $\mathcal{D} = (\mathcal{E}, \mathbb{1})$  has classical memory, according to the identifications in Eq. (A2) this implies that  $\mathcal{E}_2 = T_{\text{corr}} = \mathbb{1}$ . In Ref. [25] a correction scheme restoring quantum information is defined exactly by the fact that  $T_{\text{corr}} = \mathbb{1}$ .

Suppose now there is a scheme correcting quantum information for  $\mathcal{E}$ , so  $T_{\text{corr}} = \mathbb{1}$ . Then, due to the *no information gain without disturbance*-theorem, every single term in the first sum in Eq. (A1) has to be proportional to the identity [25]. This can only be satisfied if  $K_{\alpha}^{\dagger} K_{\alpha} = p_{\alpha} \mathbb{1}$  such that the map has to be a convex mixture of unitary dynamics and is hence of the MU type.

Now, finally assume  $\mathcal{E}$  is MU such that the Kraus operators are proportional to  $U_{\alpha}$ . Choosing  $\mathcal{F}_{\alpha}[\rho] = U_{\alpha}^{\dagger} \rho U_{\alpha}$  we find

$$\sum_{\alpha} \mathcal{F}_{\alpha} \circ I_{\alpha} = \sum_{\alpha} p_{\alpha} U_{\alpha}^{\dagger} (U_{\alpha} \rho U_{\alpha}^{\dagger}) U_{\alpha} = \rho, \quad (\text{A3})$$

where we used that the  $U_{\alpha}$  are unitary and the  $p_{\alpha}$  sum up to one. It hence follows that for a mixed-unitary map  $\mathcal{E}$  the dynamics  $\mathcal{D} = (\mathcal{E}, \mathbb{1})$  has classical memory [25, 34]. Hence, the three statements above are equivalent and the theorem is proven.  $\square$

## Appendix B: Corollary

Note that Th. 1 is equivalent to the following Corollary:

**Corollary 1.** *A unital map  $\mathcal{E}_u$  is mixed-unitary if and only if the dynamics  $\mathcal{D} = (\mathcal{E}_u, \mathcal{E}_0)$  has classical memory for all choices of  $\mathcal{E}_0$ .*

*Proof.*  $\Rightarrow$ : This is trivial since  $\mathbb{1}$  is one particular choice for  $\mathcal{E}_0$ .

$\Leftarrow$ : This is also quite intuitive. Suppose  $\mathcal{D} = (\mathcal{E}, \mathbb{1})$  has classical memory. Then the dynamics  $\mathcal{D} = (\mathcal{E}, \mathcal{E}_0)$  also only requires classical memory.

$$\mathcal{E}_0 = \mathcal{E}_0 \circ \mathbb{1} \quad (\text{B1})$$

$$= \mathcal{E}_0 \left[ \sum_{i=1}^r \mathcal{F}_i \left[ K_i \rho K_i^{\dagger} \right] \right] = \sum_{i=1}^r \tilde{\mathcal{F}}_i \left[ K_i \rho K_i^{\dagger} \right]. \quad (\text{B2})$$

where we used the linearity of CPT maps and defined  $\tilde{\mathcal{F}}_i = \mathcal{E}_0 \circ \mathcal{F}_i$ . This result is precisely the definition of classical memory and thus we have shown that if the identity can be reached with classical memory no further memory is necessary to reach any other map  $\mathcal{E}_0$ .  $\square$

## Appendix C: Tightness of criterion (5) for $\mathcal{E}_2 = \mathbb{1}$

For  $\mathcal{E}_2 = \mathbb{1}$ , the Choi state  $E_2$  is maximally entangled and, thus, the rhs of Eq. (5) is maximal. Accordingly, the criterion is always satisfied unless the entanglement of assistance on the lhs also reaches this maximum. This is the case if and only if  $E_1$  is a mixture of maximally entangled states, which, in turn, is equivalent to  $\mathcal{E}_1$  being a MU channel [44, 45, 55].

Note that for  $\mathcal{E}_2 \neq \mathbb{1}$ , the criterion (5) is, in general, only sufficient but not necessary.

## Appendix D: Relaxed witnesses

Adapting results for quantum memory witnesses [35], we can define weaker but computationally cheaper witnesses for non-MU channels.

$$\begin{aligned} w &= \min_{W, P} \text{tr}[W E_u] + \langle \Phi^+ | P | \Phi^+ \rangle \\ \text{s.t.: } W &\otimes \frac{\mathbb{1}}{d} + P^{AC'} \otimes \Phi_+^{B'B} \\ &= Q^{AB'BC'} + (R^{AB'BC'})^{\top}_{BC'} \\ Q, R &\succeq 0, \\ W, P &\text{ Hermitian.} \end{aligned} \quad (\text{D1})$$

If  $w < 0$ , the channel  $\mathcal{E}_u$  with Choi state  $E_u$  is non-MU. A computationally even more favorable version  $w_R$  can be constructed by setting  $Q = 0$  in Eq. (D1).

In an experimental setting, only the Hermitian operator  $W$  needs to be measured in order to confirm the non-MU nature of a unital channel. No full process tomography is necessary. Moreover, the form of  $W$  can be constraint to only contain observables that are measurable in a given experimental setup.

## Appendix E: Non-convexity of the set of non-MU channels

*Proof.* Let us consider the fully depolarizing channel  $\mathcal{E}_{\text{D}}[\rho] := \sum_{i=1}^9 U_i \rho U_i^{\dagger} / 9$  given in terms of the nine unitary

Kraus operators

$$\begin{aligned} U_1 = \mathbb{1}, U_2 = Y, U_3 = Z, U_4 = Y^2, U_5 = YZ \\ U_6 = Y^2Z, U_7 = YZ^2, U_8 = Y^2Z^2, U_9 = Z^2, \end{aligned} \quad (\text{E1})$$

where

$$Y = \begin{pmatrix} 0 & 1 & 0 \\ 0 & 0 & 1 \\ 1 & 0 & 0 \end{pmatrix}, \quad Z = \begin{pmatrix} 1 & 0 & 0 \\ 0 & \omega & 0 \\ 0 & 0 & \omega^2 \end{pmatrix}, \quad (\text{E2})$$

with  $\omega = \exp(2\pi i/3)$ , which is thus easily identified as a mixed-unitary channel. We can, however, also describe this channel as a convex combination of non-mixed-unitary channels. Note that whenever  $\mathcal{E}$  is non-MU, the channel  $\mathcal{E}' = \mathcal{E} \circ U$  is also non-MU, if  $U$  is a unitary map. Using the Landau-Streater channel from Eq. (14) as the channel  $\mathcal{E}$  we can define

$$\mathcal{E}_i = \mathcal{E} \circ V_i \quad (\text{E3})$$

with  $V_i[\rho] := U_i\rho U_i^\dagger$ . The convex mixture of these  $\mathcal{E}_i$  with  $p_i = 1/9$  yields the fully depolarizing channel

$$\sum_i^9 p_i \mathcal{E}_i[\rho] = \mathcal{E} \left[ \sum_i p_i U_i \rho U_i^\dagger \right] \quad (\text{E4})$$

$$= \mathcal{E}[\mathcal{E}_D[\rho]] = \mathcal{E}_D[\rho]. \quad (\text{E5})$$

The last equality uses the fact that the fully depolarizing channel  $\mathcal{E}_D[\rho] = \mathbb{1}$  for all  $\rho$  and that  $\mathcal{E}$  is unital.  $\square$

### Appendix F: Details on the investigated qutrit channels

The fully depolarizing channel of a qutrit  $\mathcal{E}_D[\rho] = \text{tr}\{\rho\}\mathbb{1}/3$  maps every state to the maximally mixed state. It is known that mixing this channel with any other unital channel as in Eq. (15) is mixed-unitary for  $p \geq 7/8$  in the qutrit case [21]. The Landau-Streater channel [16, 17], which, in the qutrit case, is related to the Werner-Holevo channel [56], is a unital qutrit channel without mixed-unitary representation. It is not only extremal in the set of unital channels but also in the set of all qutrit channels.

There are also unital qutrit channels without mixed-unitary representations which are extremal unital channels but not extremal in the set of all channels. Two known examples are the Arveson-Ohno channel  $\mathcal{E}_{AO}$  and a family constructed by Haagerup, Musat and Ruskai. Both have in common that they are rank-4 channels. One representation of the Arveson-Ohno channel  $\mathcal{E}_{AO}$  is given by [18]

$$\begin{aligned} K_1 = |0\rangle\langle 0|, \quad K_2 = |0\rangle\langle 1| + \sqrt{2}|1\rangle\langle 2| \\ K_3 = \sqrt{2}|1\rangle\langle 0| + \sqrt{3}|2\rangle\langle 1|, \quad K_4 = |2\rangle\langle 0| + \sqrt{2}|0\rangle\langle 2|. \end{aligned} \quad (\text{F1})$$

The family  $\mathcal{E}_{\text{HMR}}(\alpha, \beta)$  is non-mixed-unitary for almost all  $\alpha, \beta \in \mathbb{C}$  with  $|\alpha|^2 + |\beta|^2 = 1$ . A Kraus representation is given by [20]

$$\begin{aligned} K_1 = \alpha|0\rangle\langle 0| + |1\rangle\langle 2|, \quad K_2 = \beta|0\rangle\langle 2| + |2\rangle\langle 1| \\ K_3 = -|0\rangle\langle 1| - \beta^*|2\rangle\langle 0|, \quad K_4 = |1\rangle\langle 0| + \alpha^*|2\rangle\langle 2|. \end{aligned} \quad (\text{F2})$$

The parameters chosen for the investigation in Tab. I are  $\alpha = 1/\sqrt{5}$  and  $\beta = 2/\sqrt{5}$ . They are chosen such that the absolute value of  $s_{\text{QM}}$  according to the SDP Eq. (9) is maximal.

### Appendix G: Performance of different witnesses

We investigated all convex combinations of the form  $\mathcal{E}_p = p\mathcal{E}_A + (1-p)\mathcal{E}_B$  with respect to the property of being non-MU. The graphical representation in Fig. 3 is based on the numerical results summarized in Tab. I. There, not only the quantum memory witness  $s_{\text{QM}}$  from Eq. (9) and the Mendl-Wolf witness  $s_{\text{MW}}$  from Eq. (16) were investigated, but also the weaker variants  $w$  and  $w_R$  of the quantum memory witness in Eq. (D1). Those require on the one hand less computing time but are on the other hand not as exact as the full quantum memory witness. In higher dimensions this may be advantageous.

$\mathcal{E}_A$	$\mathcal{E}_B$	$s_{\text{QM}} < 0$	$w < 0$	$w_R < 0$	$s_{\text{MW}} < 0$
$\mathbb{1}$	$\mathcal{E}_{\text{LS}}$	$p < 1$	$p < 1$	$p < 1$	$p < 0.33$
$\mathcal{E}_D$	$\mathcal{E}_{\text{LS}}$	$p < 0.5$	$p < 0.5$	$p < 0.02$	$p < 0.5$
$\mathcal{E}_{\text{AO}}$	$\mathcal{E}_{\text{LS}}$	$\forall p$	$p < 0.50$	$p < 0.08$	$p < 0.51$
$\mathcal{E}_{\text{HMR}}$	$\mathcal{E}_{\text{LS}}$	$\forall p \setminus [0.89, 0.91]$	$\forall p \setminus [0.89, 0.91]$	$p < 0.07$	$p < 0.63$
$\mathbb{1}$	$\mathcal{E}_{\text{AO}}$	$p < 0.08$	$p < 0.08$	$p = 0$	-
$\mathcal{E}_D$	$\mathcal{E}_{\text{AO}}$	$p < 0.18$	$p < 0.18$	$p = 0$	-
$\mathcal{E}_{\text{HMR}}$	$\mathcal{E}_{\text{AO}}$	$\forall p \setminus [0.71, 0.94]$	$\forall p \setminus [0.69, 0.96]$	$p = 0$	-
$\mathcal{E}_D$	$\mathcal{E}_{\text{HMR}}$	$p < 0.03$	$p < 0.02$	-	-
$\mathbb{1}$	$\mathcal{E}_{\text{HMR}}$	$p < 1$	$p < 1$	-	-

Table I. Overview of the performance of the different non-MU witnesses in the convex combinations of the five selected unital qutrit channels. The investigated families take the form  $\mathcal{E}_p = p\mathcal{E}_A + (1-p)\mathcal{E}_B$  and the cells of the table contain the parameter ranges of  $p$  for which  $\mathcal{E}_p$  being non-MU can be certified with the according witness.